Received: 18 April 2022 | Revised: 10 July 2022 | Accepted: 11 July 2022

DOI: 10.1002/apj.2813

RESEARCH ARTICLE

Asia-Pacific Journal of Chemical Engineering | Curtin University | WILEY

Experimental study on seepage flow characteristics of leaked molten salt in foundation fillers in concentrating solar power plants

Mingrui Zhang | Yuhang Zuo | Xinfeng Yu | Ao Zhang | Hao Zhou

State Key Laboratory of Clean Energy Utilization, Institute for Thermal Power Engineering, Zhejiang University, Hangzhou, China

Correspondence
Hao Zhou, State Key Laboratory of Clean Energy Utilization, Zhejiang University, Zheda Road 38, Hangzhou 310027, China.
Email: zhouhao@zju.edu.cn

Funding information
National Natural Science Foundation of China, Grant/Award Number: 52036008

Abstract

The leakage of molten salt storage tanks in concentrating solar power plants has attracted much attention. This paper focused on seepage and migration characteristics of molten salt in the thermal-steady foundation fillers with different configurations after leakage occurs through a self-built experimental system modeling the actual leaking process. The results show that the thermal insulation of light expanded clay aggregate (LECA) as foundation fillers is better than that of sand and gravel. When the operating temperature is 565°C, the average temperatures of each layer of LECA, sand, and gravel are 131.73°C, 141.91°C, and 149.27°C, respectively. And the seepage depths in light expanded clay aggregate, sand, and gravel are 482 mm, 223 mm, and 270 mm, respectively. It is found that the seepage depth of molten salt distinctly increases with higher operating temperature in all kinds of fillers. Nevertheless, the seepage depth of molten salt in the multi-layer fillers diminishes with the increase of the thickness of the sand or gravel layer. The results obtained from this research would be helpful for the engineering design of storage tank foundations and reduce economic losses and the complexity of accident handling.

KEYWORDS

concentrating solar power, foundation fillers, molten salt leakage, seepage

1 | INTRODUCTION

With the rapid economic development, the consumption of traditional fossil energy is increasing, and the global energy-related CO_2 emissions in 2020 reach as high as 31.5 Gt per year.[1] The level of CO_2 emission has been confirmed to be related to global warming, climate change, and environmental degradation, and poses a significant challenge to the human living environment. The large-scale application of clean energy can effectively reduce carbon dioxide emissions and play an essential role in achieving "carbon neutrality".[2,3] During the past decades, concentrating solar power (CSP) has gained significant attention as a renewable energy power generation method due to its cleanness and efficiency, energy storage and peak shaving, and continuous power generation.[4,5] According to the International Renewable Energy Agency statistics, cumulative CSP installed capacity grew just over fivefold globally between 2010 and 2020, reaching around 6.5 GW at the end of 2020.[6]

During the operation of the CSP plants, the heliostats concentrate the solar energy on the heat receiver. The molten salt in the receiver is heated by solar energy and

then guided to the molten salt heat storage device or power circulation device.[7] The storage tank is an integral part of the thermal energy storage system (TESS) in the CSP plant. The unreasonable design of the storage tank may make the molten salt cool to the freezing point, which seriously threatens the safe operation of the power plant. Therefore, storage tank heat loss and its optimal design have become the focus of many researchers. Herrmann et al.[8] evaluated the technical and economic feasibility of dual-tank molten salt storage and performed a regression analysis on the heat loss measurements of the Solar Two power plant to derive an empirical heat loss equation. Zaversky et al.[9] built a fully transient tank model and successfully compared it with the heat loss data observed in practical molten salt storage tanks. It was found that heat loss can be affected significantly by the external surface temperature of the tank, absorbed solar radiation, and ambient air temperature. Rodríguez et al.[10] proposed a modular object-oriented approach to solve the molten salt storage tank problem by treating the different elements as independent systems. To study the cooling process of the state-of-the-art molten salt thermal storage tanks during these standby periods, Suárez et al.[11] developed a computational fluid dynamics model. The results show that the tank filling level has a significant effect on the onset of localized crystallization. Bonilla et al.[12] proposed a dynamic tank model and validated it against experimental data under static heat loss estimation, charging, and discharging processes. Araújo et al.[13] proposed a transient model of heat loss from the storage tank to the environment, discussing the effect of climatic conditions, load levels, and operating temperature on heat loss from the CSP heat storage system. Torras et al.[14] used a modular object-oriented approach to study the effect of meteorological data, the insulation thickness of the tank, and the configurations of the foundation on the heat loss.

As a part of the whole storage system, the molten salt storage tank foundation not only plays the role of supporting the tank body but also needs to reduce the heat loss from the tank and prevent the overheating of a concrete building structure. If the soil overheats, it can dry out, which can cause the tank to settle. If concrete overheats, it can lose strength and cause foundation damage. The foundation design used at Solar Two worked well, but it was expensive. The simplified and inexpensive foundation uses expanded clay as insulation instead of foam glass and refractory materials.[15] Zhou et al.[16,17] studied the porous structure, thermal properties, permeability, and compressive strength of the stacked ceramsite used in the foundation materials of the storage tank in the solar thermal power plant. A new type of foundation structure was proposed to insulate the storage tank, and the temperature distribution and heat loss of the foundation at different kinds of scales were also investigated. The results show that the thermal performance of the foundation can be improved, and the heat loss through the foundation can be reduced by using expanded clay and changing the configurations of the tank foundation. Due to the influence of the foundation of the storage tank, the enormous thermal stress generated by uneven temperature may cause mechanical deformation of the storage tank, and even cause the storage tank to rupture and cause molten salt leakage accidents. The Gemasolar CSP plant in Seville, Spain, which can generate electricity 24 h a day, was shut down due to the molten salt tank accident in 2017. Due to the severe damage, the original tank body needs to be dismantled to rebuild the tank. Roughly estimated, the repair cost will be around 9 million euros, and the loss of electricity sales revenue caused by the power plant's shutdown is even greater. To have a clearer understanding of the causes of storage tank leakage and better prevention and treatment, many researchers have made efforts. Wan et al.[18] proposed a coupled thermal performance evaluation model to evaluate storage tanks' heat loss and temperature distribution. It is found that lower tank foundation stiffness can reduce the maximum stress of the tank. Zhou et al.[19] explored a series of influencing factors on the seepage and solidification process of molten salt in the thermal porous system after a tank leakage accident through a self-designed experimental system. Shi et al.[20] explored the migration characteristics of molten salt which leaked through the crack in thermally stable foundation materials and obtained the seepage range under different working conditions. The results showed that there is little effect of crack length and width on migration depth that impact the agglomeration morphology made of the solidified salt and porous foundation materials directly. Wang et al.[21] studied the thermophysical properties of the accumulated ceramsite in the tank foundation with three different particle size ratios after the leakage of molten salt using three-dimensional volume reconstruction from X-ray microtomography technology. It is found that the thermal conductivity increased by 4.0 to 5.0 times after molten salt leakage leading to a substantial increase in the heat loss.

Combining the above research, the overall performance of the foundation is crucial for the operation safety of the molten salt storage tank. And it can be found that research on molten salt leakage mainly focuses on the molten salt seepage characteristics in expanded clay. However, types of fillers are not limited to expanded clay in the practical tank foundation. There is little research on the seepage and solidification

characteristics of molten salt in various fillers. In this paper, a comparative experimental study on the molten salt seepage characteristics in three types of foundation fillers, including light expanded clay aggregate (LECA), sand, and gravel, was carried out. Meanwhile, the seepage process of the leaked molten salt in the lab-scale and practical foundation fillers was also explored. The research results will help guide the selection of storage tank foundation fillers, which has essential engineering significance to the safe operation of the molten salt TESS of the CSP plants and the design of the storage tank foundations.

2 | MATERIALS AND METHODS

2.1 | Experimental materials

The molten salt used in the experiments is Solar Salt[22,23] supplied by Zhejiang Lianda Chemical Company Limited, China. The salt is a mixture of $NaNO_3$ and KNO_3 in 60:40 wt % ratio, and its properties are shown in Table 1.[19] The foundation fillers used are LECA, sand, and gravel, respectively. Among them, sand and gravel have enough rigidity to keep the floor around the foundation flat but have high thermal conductivity.[24,25] LECA can effectively prevent the foundation from heat loss, but its porous structure makes it fragile and prone to settlement. The images of the three types of foundation fillers are shown in Figure 1. And the characteristics of fillers including particle sizes, packed bulk density, and porosity are shown in Table 2.

TABLE 1 Property of solar salt[19]

Properties	Unit	Value (T, °C)
Melting point	°C	220.85
Freezing point	°C	237.85
Latent heat	kJ/kg	113.03
Specific heat	J/(kg·°C)	1,443 + 0.172·T
Density	kg/m^3	2090–0.636·T
Thermal conductivity (liquid state)	W/(m·K)	0.443 + 0.00019·T

2.2 | Experimental system

In order to model the actual molten salt seepage process in the foundation fillers after the leaking of storage tanks, the leakage and seepage experiment system of the molten salt was built, as shown in Figure 2. The experimental system comprises a test rig, resistance heater, temperature control instrument, lifting device, muffle furnace, computer, data acquisition instrument, and thermocouples.

The muffle furnace can heat the molten salt used in the experiment to the required temperature. The complex molten salt storage tank is replaced by an electrical resistance heater with a temperature control range from 30°C to 800°C, which implements the thermal effect of high-temperature molten salt in the tank on the foundation materials. The test rig has a cylindrical shape with an inner diameter of 345 mm and a depth of 760 mm, and the height of the heater is 60 mm. The interior of the test rig is filled with foundation fillers. And the walls of the test rig and electrical resistance heater are insulated by refractory bricks and aluminosilicate fiber cotton to reduce heat

TABLE 2 Characteristics of fillers

Parameters	LECA	Sand	Gravel
Particle size (mm)	3–5		
Packed bulk density (kg/m^3)	474.05	1417.47	1623.31
Porosity (%)	37.90	45.46	42.84

(a) LECA (b) Sand (c) Gravel

FIGURE 1 Foundation fillers of storage tank

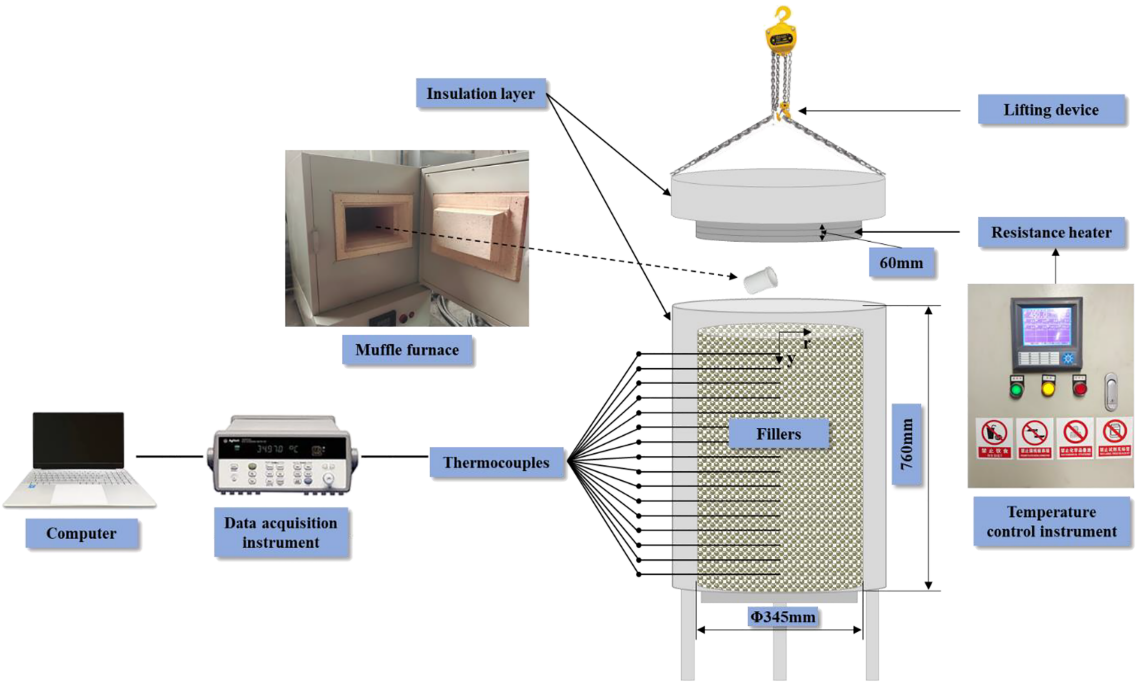

FIGURE 2 Experimental system of molten salt seepage

dissipation during the experiment. The bottom tray of the test rig can be opened to discharge the filling foundation materials. A total of 15 K-type thermocouples are arranged every 40 mm along the axial direction of the tank center with an accuracy of ±1°C. The thermocouples can measure the temperature change and distribution of foundation materials during the experiment. All the thermocouples are connected to the data acquisition instrument. And the data can be read and saved on the computer.

2.3 | Experimental methods

The experimental procedures include molten salt pretreatment process, foundation fillers heating process, molten salt leakage process, and data measurement process.

1) First, heat the salt in at 110°C for 5 h for drying treatment, weigh the required mass of salt, and put it into the crucible. After setting the heating program of the muffle furnace, put the crucible into the muffle furnace.

2) Pull up the heater, pour the foundation fillers into the test rig, and then put down the heater. Use the temperature control device to set the temperature of the resistance heater, then turn on the resistance heater and heat until the temperature change of the foundation fillers within 3 h shall not exceed 0.5°C. At this point, the temperature of fillers is considered to have reached a steady state.

3) Pull up the resistance heater, take out the crucible containing molten salt from the muffle furnace, pour the molten salt into the foundation fillers at the central position, and then quickly put down the heater. Continue to maintain the heater temperature, pull out the thermocouples after 0.5 h so as to prevent the molten salt from sticking to the thermocouples after solidification and unable to remove the solid blocks, and then turn off the heater after another 10 h.

4) After the foundation fillers are cooled, pull up the heater and open the bottom tray of the test rig to release the fillers, take out the molten salt fillers, solid blocks formed after the molten salt solidifies in the foundation fillers, measure, and record the corresponding experimental data.

The experimental cases are shown in Table 3. Cases A1–A4, B1–B4, and C1–C4 compare the seepage characteristics of molten salt in LECA, sand, and gravel at different operating temperatures, respectively. These cases above are all studied on the seepage characteristics of molten salt in single-layer fillers. In contrast, the seepage characteristics of molten salt in multi-layer fillers are studied in cases E1–E3. The multi-layer fillers configuration in case E2 refers to Zhou et al.[16] The multi-layer fillers configuration in case E3 refers to the foundation fillers of a practical CSP plant and is arranged in equal proportions. Figure 3 is a schematic

TABLE 3 Conditions of cases

Case	Configuration of foundation fillers	Operating temperature T_{op}/°C
A1	LECA	565
A2	LECA	500
A3	LECA	400
A4	LECA	290
B1	Sand	565
B2	Sand	500
B3	Sand	400
B4	Sand	290
C1	Gravel	565
C2	Gravel	500
C3	Gravel	400
C4	Gravel	290
E1	$a = 250$ mm, $b = 0$ mm, $c = 450$ mm	565
E2	$a = 60$ mm, $b = 175$ mm, $c = 465$ mm	565
E3	$a = 10$ mm, $b = 120$ mm, $c = 570$ mm	565

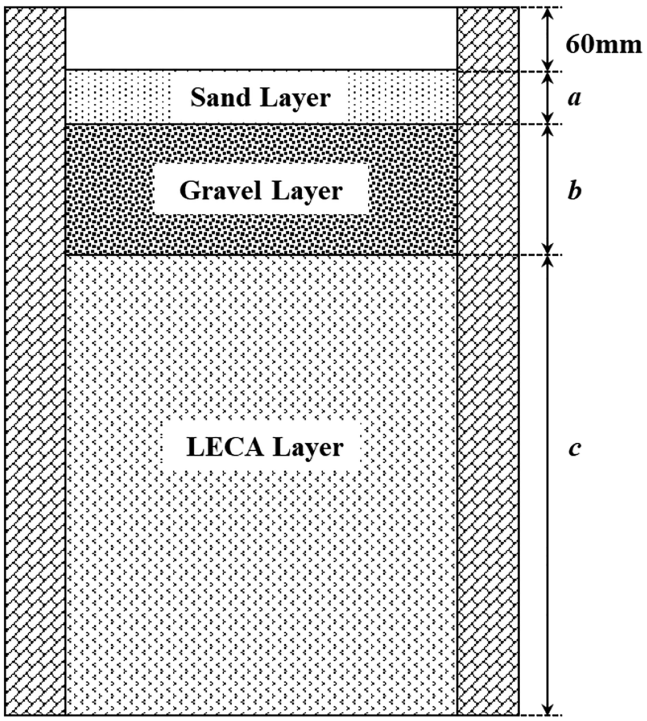

FIGURE 3 Schematic diagram of the layout of the multi-layer fillers

diagram of the layout of the multi-layer fillers. It can be seen that the top of the foundation is the sand layer, the middle is the gravel layer, and the bottom is the

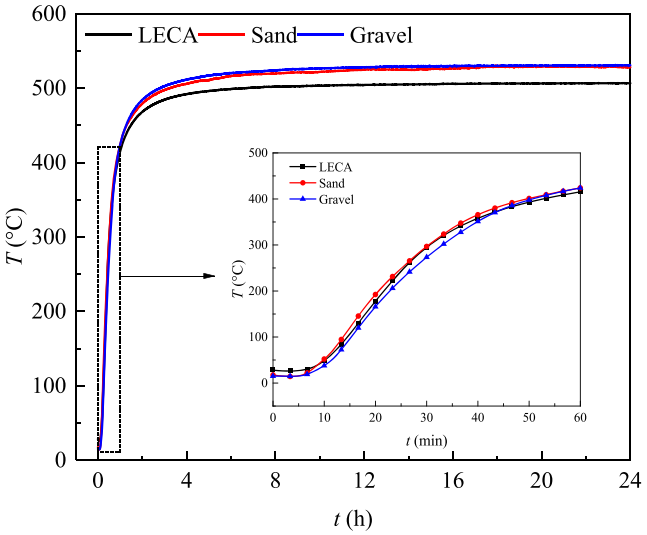

FIGURE 4 The temperature rise of foundation fillers during the heating process

LECA layer. a is the thickness of the sand layer, b is the thickness of the gravel layer, and c is the thickness of the LECA layer.

3 | RESULTS AND DISCUSSION

3.1 | Temperature evaluation of foundation fillers in the heating process

The temperature rise at $y = 40$ mm during the heating process in LECA, sand, and gravel for 24 h when the operating temperature T_{op} is 565°C is shown in Figure 4, and the corresponding cases are A1, B1, and C1, respectively. It can be seen from Figure 4 that in the first 5 min of heating, the temperature basically did not change, probably because the heat had not been conducted to the position of $y = 40$ mm. In the 5–10 min interval, the temperature began to rise significantly, but the rising speed was relatively slow. The temperature of each kind of filler rose rapidly within the time interval of 10–40 min and was heated from about 50°C to 350°C. In the time interval of 40–60 min, although the temperature continued to rise, the temperature rise rate decreased compared with the previous period. After heating for 1 h, the temperatures of LECA, sand, and gravel at the position of $y = 40$ mm were 411.41°C, 419.67°C, and 419.41°C, respectively. The rate of temperature rise became very slow after 6 h of heating. After 24 h of heating, the temperature of the three fillers reached a steady state, and the temperatures at $y = 40$ mm of LECA, sand, and gravel were 506.63°C, 528.91°C, and 531.32°C, respectively.

3.2 | Temperature distribution of foundation fillers in steady state

The steady-state temperature distribution of each kind of foundation filler is shown in Figure 5. This allows the conclusion that with the increase of operating temperature, the temperature of each layer of the foundation increases. When the operating temperatures T_{op} are 290°C, 400°C, 500°C, and 565°C, the average temperatures of each layer of LECA foundation are 67.69°C, 88.91°C, 115.99°C, and 131.73°C, respectively; the average temperatures of each layer of the sand foundation are 76.90°C, 101.19°C, 128.63°C, and 141.91°C, respectively; the average temperatures of each layer of the gravel foundation are 76.76°C, 99.15°C, 127.27°C, and 149.27°C, respectively. As the depth position of fillers y increases, the temperature distinctly decreases, and the temperature gap among different operating temperatures gradually narrows. The temperature difference of the upper layer of the foundation ($y \leq 320$ mm) is large, and that of the lower layer ($y > 320$ mm) is slight at different operating temperatures. This is mainly because the thermal insulation in the horizontal direction of the test rig is not very good. In the process of heat transfer, the horizontal dissipation is severe.

Since the practical operating temperatures of the cold and hot salt tanks of the power plants are 290°C and 565°C, respectively, the temperature distributions of the different foundation fillers at these two operating temperatures are selected for comparison, shown in Figure 6. When the operating temperature T_{op} is 565°C, the temperatures of the foundation fillers LECA, sand, and gravel at $y = 40$ mm are 506.63°C, 528.91°C, and 531.32°C, respectively, and the average temperatures of the upper layer ($y \leq 320$ mm) of the foundation are 218.28°C, 235.01°C, and 245.22°C, respectively. When the operating temperature T_{op} is 290°C, the temperatures of the foundation fillers LECA, sand, and gravel at $y = 40$ mm are 257.78°C, 254.99°C, and 276.58, respectively, and the average temperatures of the upper layer ($y \leq 320$ mm) of the foundation are 105.56°C, 117.96°C, and 121.60°C, respectively. It can be seen from the above that when sand and gravel are used as foundation fillers, the thermal insulation is poor, and the temperature level of the storage tank foundation is relatively high. However, sand and gravel are of higher flatness and can also provide higher strength to the foundation. LECA can better meet the thermal insulation requirements of the foundation, mainly because the porous structure inside the LECA makes the thermal conductivity lower and the thermal insulation better.[26] Therefore, it is not appropriate to use sand or gravel as all fillers in the practical storage tank foundation. Otherwise, it will increase the heat

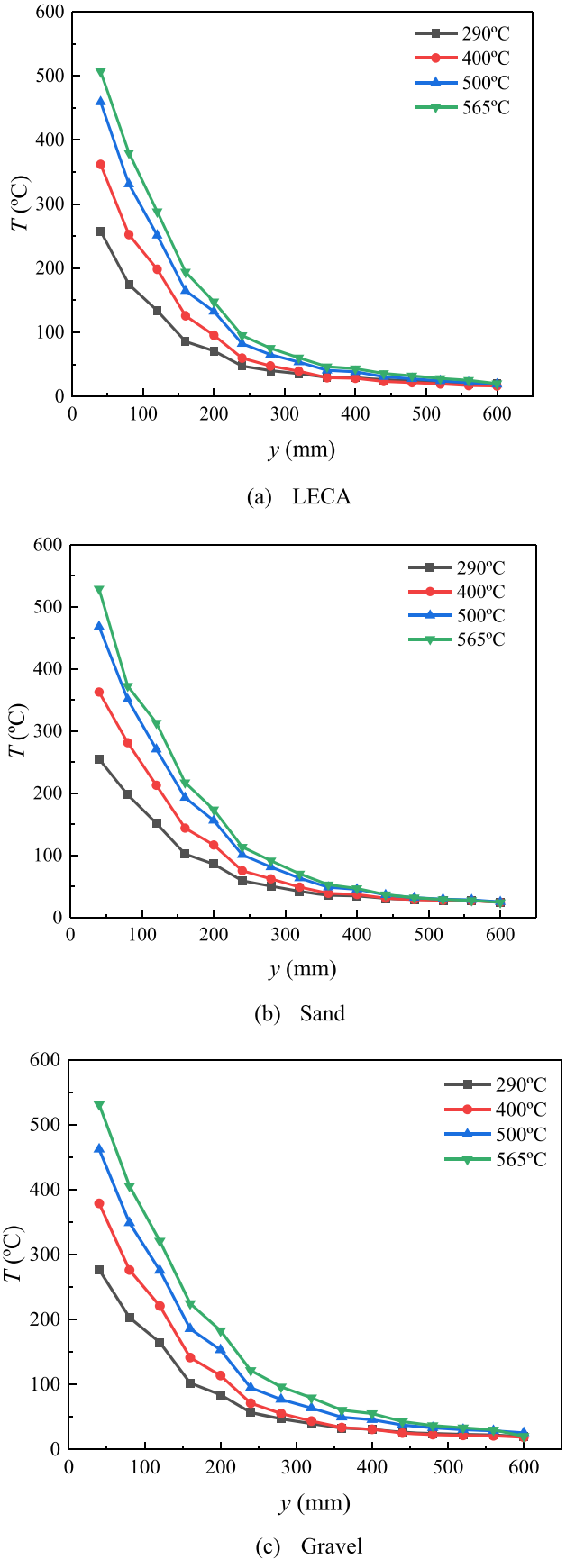

FIGURE 5 Steady-state axial temperature distribution at different operating temperatures

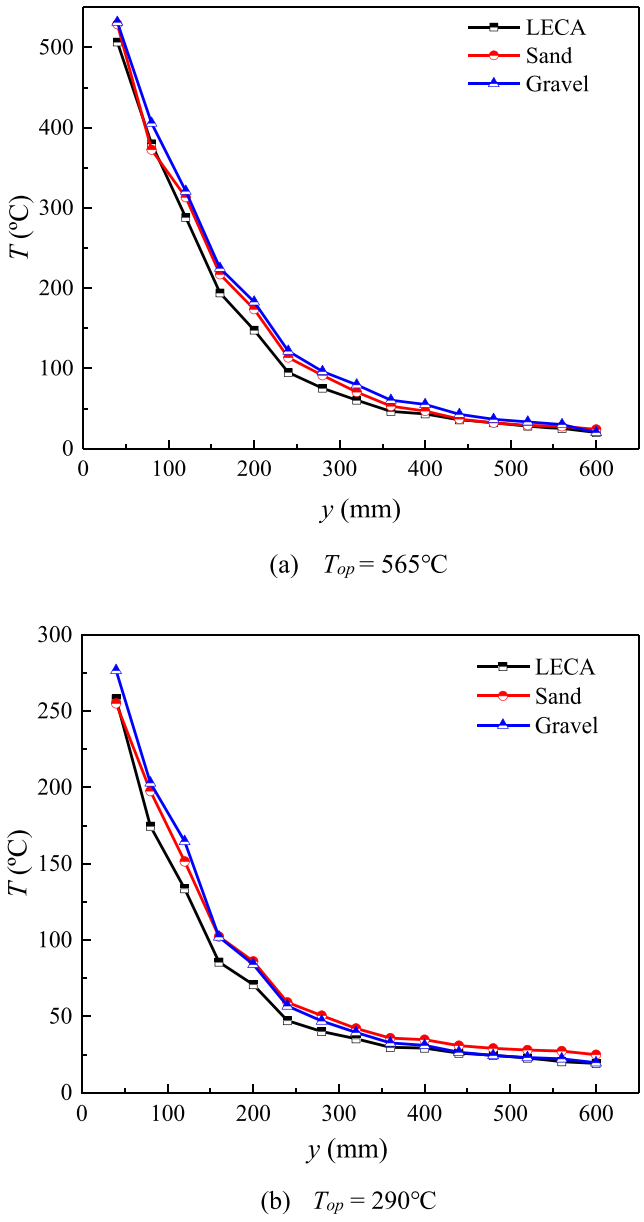

(a) T_{op} = 565°C

(b) T_{op} = 290°C

FIGURE 6 Steady-state axial temperature distribution of different foundation fillers

loss of the storage tanks and endanger the safe operation of the CSP plants.

3.3 | Seepage characteristics in foundation fillers

3.3.1 | Seepage characteristics of molten salt in single-layer fillers

Figure 7 shows the seepage characteristics of molten salt in each kind of foundation filler. When T_{op} is 565°C, 500°C, 400°C, and 290°C, the seepage depths D of molten

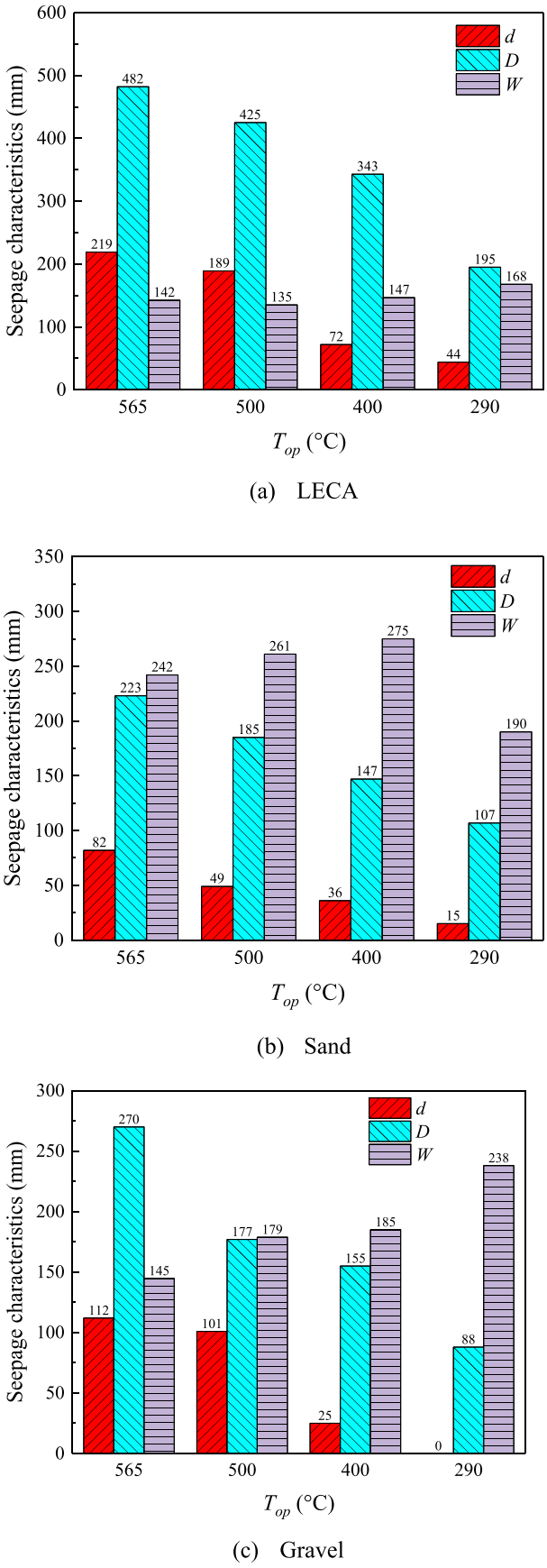

(a) LECA

(b) Sand

(c) Gravel

FIGURE 7 Seepage characteristics of molten salt at different operating temperatures

salt in LECA are 482 mm, 425 mm, 343 mm, and 195 mm, respectively; the seepage depths of molten salt in sand are 223 mm, 185 mm, 147 mm, and 107 mm, respectively; and the seepage depths of molten salt in gravel are 270 mm, 177 mm, 155 mm, and 88 mm, respectively. The operating temperature significantly affects the seepage depth (D) and the distance between the top of the solid block and the top of the fillers (d). D and d diminish with the decrease of operating temperature. This is mainly because when T_{op} is high, the temperature of the upper layer of the fillers is also high. The position in the foundation where the temperature is lower than the freezing point of the molten salt is deeper so that the molten salt is not easy to solidify and crystallize in the upper part of the foundation. Finally, the seepage depth is more prominent. The variation law of maximum seepage width W with temperature is not apparent, but it can be concluded that W in sand and gravel is obviously higher than that in LECA. Excessive seepage width may cause the molten salt to adhere to the inner wall of the foundation, which is very unfavorable for accident handling because the formed sticking part is very hard. In the practical system operation, due to the more intense molten salt corrosion and the thermal stress caused by the huge temperature difference, the hot salt tank is more likely to rupture and cause molten salt leakage. Therefore, it is necessary to focus on protecting the hot salt tank to prevent accidents. Otherwise, the processing will be more complex, and the economic loss will be heavier.

Figure 8 compares the seepage depth of molten salt in the foundation fillers at different operating temperatures. It can be clearly seen that when the operating temperature T_{op} is the same, the seepage depth of molten salt in LECA is much higher than that of gravel and sand. When T_{op} is 565°C, the seepage depth of molten salt in LECA is 116.14% and 78.52% higher than that in sand and gravel, respectively. The seepage depth in LECA is significantly increased, which will also deepen the difficulty of dealing with the leakage accident of the storage tank. According to the research results in Zhou et al.,[19] the greater the porosity of the fillers, the greater the seepage depth should be. Nevertheless, it can be seen from Table 2 that the porosity of LECA, sand, and gravel are 37.90%, 45.46%, and 42.84%, respectively, while the seepage depth of molten salt in different fillers has no apparent correlation with the porosity. This shows that the seepage depth of molten salt in the fillers is the result of a combination of factors. As far as this study is concerned, this is because the sand and gravel have better thermal conductivity and undergo intense heat transfer with the molten salt during the seepage process. The faster the molten salt cools, the earlier the phase change occurs, preventing the molten salt from continuing to seep downward. Meanwhile, the shape of sand and gravel is flatter; while LECA is similar to a spherical shape, the gap sizes between particles of LECA are larger. And the seepage resistance of molten salt in LECA is more negligible, so the seepage depth of molten salt in LECA is higher than that of molten salt in sand and gravel.

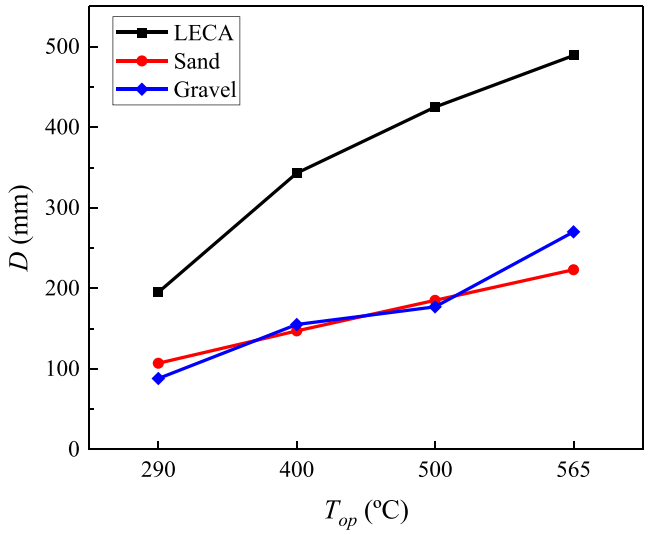

FIGURE 8 Seepage depths of molten salt in three kinds of foundation fillers

The solid blocks formed after the molten salt seepage and phase change in the foundation fillers are shown in Figure 9. The widths of the top of molten salt-LECA solid blocks are smaller than that of the bottom, and a large amount of molten salt has accumulated at the bottom of the solid block. On the other hand, the situation of molten salt-gravel solid blocks and molten salt-sand solid blocks is opposite to that of molten salt-LECA solid blocks. The widths of the top are larger than that of the bottom, but the molten salt also accumulates in a large amount at the bottom of the solid blocks. This may be because the seepage resistance of LECA to molten salt is small. During the seeping process, the molten salt rapidly migrates downward and does not tend to migrate horizontally due to the action of gravity. Solidification occurs when the molten salt reaches the position with the lower temperature at the bottom of the foundation. The molten salt above cannot make solid crystals at the bottom melt and break through, and it can only diffuse and migrate horizontally. Therefore, the bottom widths of molten salt-LECA solid blocks are larger. However, the seepage resistance of gravel and sand to molten salt is relatively large. At the beginning of the seepage process, the molten salt above does not have the disposition to continue to seep downward. Meanwhile, due to the advance of the

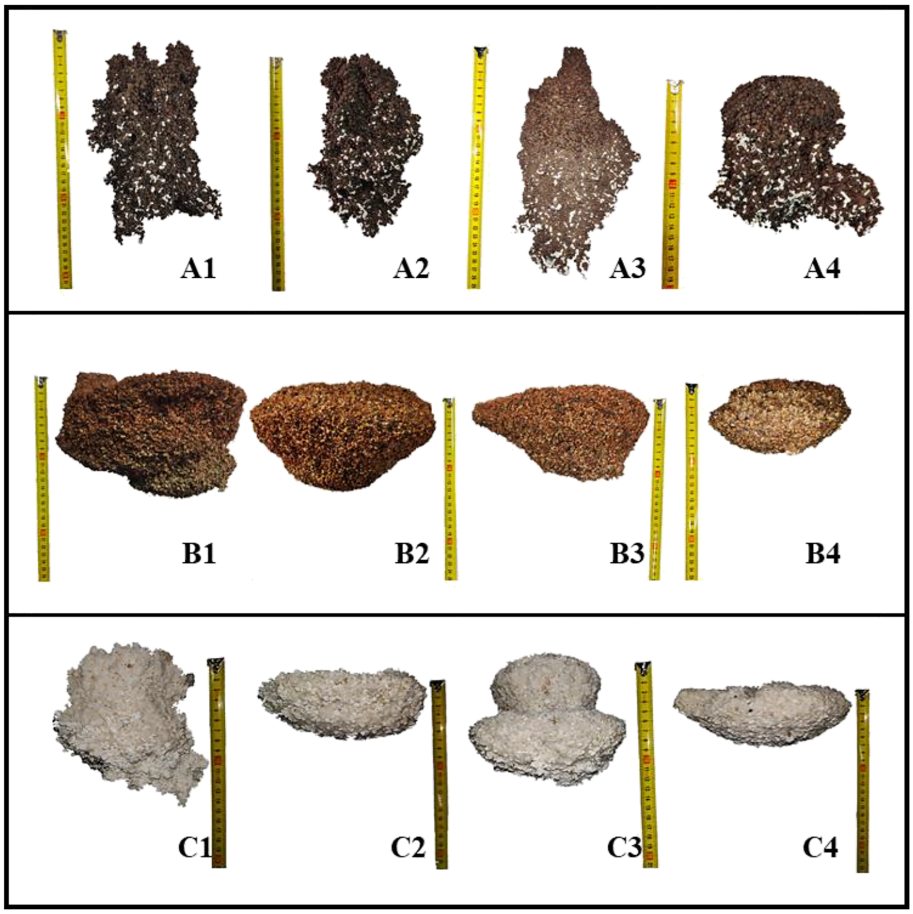

FIGURE 9 Moten salt-fillers solid blocks

solidification position, the molten salt cannot continue to seep downward but can only seep in the horizontal direction. Because of the higher temperature in the horizontal direction of the upper layer, the molten salt solidifies more slowly here. Eventually, solid blocks with the shape of a cone are formed. When a leakage accident occurs in a practical CSP plant, the thermal conductivity of the solid blocks formed by the molten salt and the foundation fillers are greatly improved. If no treatment is carried out after the accident, the heat loss of the storage tank foundation will be greatly increased, which is not conducive to the safe operation of the molten salt storage tank. Therefore, the solid blocks formed by the molten salt and the foundation fillers should be dug out and cleaned up after the accident. The smaller seepage depth and seepage width of the molten salt in the foundation fillers mean easier accident handling. It can be concluded that when sand and gravel are used as foundation fillers, it may be easier for CSP plants to deal with leakage accidents.

The temperature change of the foundation fillers within 1400 s after the molten salt leakage of case C1 is shown in Figure 10. Noteworthy is the fact that the seepage depth of molten salt in the gravel reaches 270 mm when the operating temperature is 565°C seen in

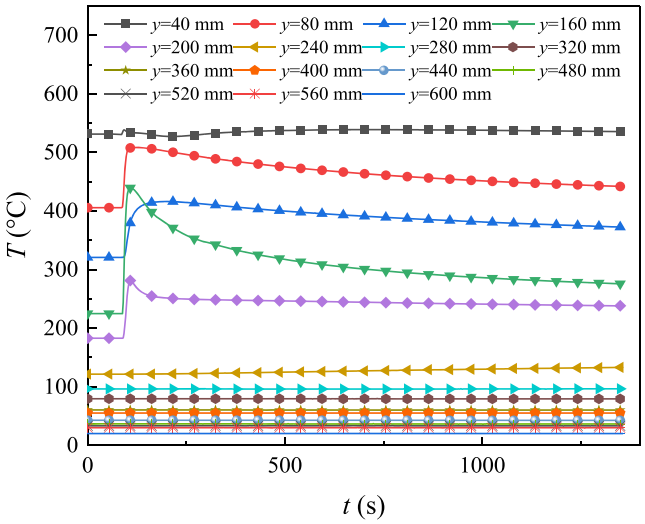

FIGURE 10 Temperature change and distribution of the foundation of case C1 (gravel foundation, $T_{op} = 565°C$)

Figure 7c, but the thermocouple at $y = 240$ mm does not detect the temperature change. It can be seen from Figure 9 that the molten salt seepage does not proceed along the central axis at the end but shifts to the

horizontal direction in case C1. The high-temperature molten salt is not in direct contact with the thermocouple, so the temperature level at the position of $y = 240$ mm does not change. It can be seen that there is considerable uncertainty in the detection of molten salt leakage by arranging thermocouples in the tank foundation. This is mainly reflected in the fact that after the leaking of the storage tank, if the molten salt does not flow through the temperature measuring point, the thermocouples cannot accurately detect the temperature change, so it is impossible to know whether the storage tank leaks. Of course, the probability of this situation can be reduced by adding temperature measuring points in the storage tank, but arranging more thermocouples in the storage tank will have an adverse effect on the structure and strength of the storage tank foundation. Therefore, research should be devoted to how to perform leak detection of molten salt storage tanks efficiently, accurately, and without disturbance in the future.

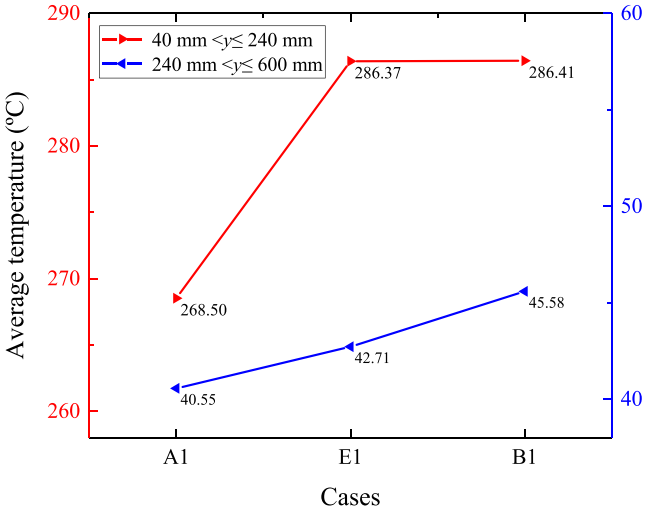

FIGURE 11 The average temperatures of the foundation of cases A1, E1, and B1

3.3.2 | Seepage characteristics of molten salt in multi-layer fillers

Combining the research results in sections 3.2 and 3.3.1, it can be found that sand can effectively reduce the seepage depth of molten salt in the foundation fillers. When T_{op} is 565°C, the seepage depth in sand is 223 mm, which is only 46.27% of the seepage depth in LECA at the same temperature. However, sand has poor thermal insulation, while LECA can prevent heat loss with validity. Therefore, a foundation configuration with sand in the upper layer and LECA in the lower layer is proposed in case E1. In this way, the sand can be used to prevent the seepage of molten salt and the LECA can be applied to insulate the tanks simultaneously. In case E1, the thickness of the sand layer a is 250 mm, and the thickness of the LECA layer c is 450 mm. The average temperatures of the foundation of cases A1, E1, and B1 are shown in Figure 11. At the position of 40 mm $< y \leq$ 240 mm, the average temperatures of cases A1, E1, and B1 are 268.50°C, 286.37°C, and 286.41°C, respectively. The average temperatures of cases E1 and B1 are almost the same. This is mainly because all the fillers in case B1 are sand, and the fillers at the position of 40 mm $< y \leq$ 240 mm in case E1 are also sand. At the position of 240 mm $< y \leq$ 600 mm, the average temperatures of cases A1, E1, and B1 are 40.55°C, 42.71°C, and 45.58°C, respectively. Although the fillers of cases A1 and E1 at the position of 240 mm $< y \leq$ 600 mm are all LECA, due to the better thermal conductivity of the sand layer in case E1, the overall temperature of the lower LECA layer is also slightly increased. However, the average temperature of case E1 is still 2.87°C lower than that of case B1 at the position of 240 mm $< y \leq$ 600 mm, which is still due to the better thermal insulation performance of LECA. Therefore, the foundation configuration with sand in the upper layer and LECA in the lower layer has better thermal insulation than the foundation configuration with all sand. However, because the thickness of the sand layer is too large, the thermal insulation effect of the LECA layer is weakened.

In practical engineering applications, considering that the foundation has to bear the massive gravity of the storage tank and molten salt, the foundation will be filled with gravel to improve the compressive strength of the foundation and prevent the settlement of the foundation. The configurations of foundation fillers in cases E2 and E3 are proportional to the lab-scale storage tank foundation and a practical storage tank foundation. Due to the high thermal insulation requirements of the actual foundation, the thickness of the LECA layer c is larger, accounting for 81.4% of the thickness of the foundation fillers. The seepage depths of molten salt in multi-layer foundation fillers in cases E1–E3 are shown in Figure 12. The thickness of the LECA layer c in cases E1, E2, and E3 are 450 mm, 465 mm, and 570 mm, respectively, and the seepage depths are 225 mm, 332 mm, and 403 mm, respectively. The main conclusion that can be drawn is that when molten salt seeps into the multi-layer fillers, the seepage depth increases with the thickness of LECA. The seepage depth of case E1 is almost the same as that of case B1, the molten salt did not infiltrate into the LECA layer, and the sand completely blocked the molten salt. The solid block of Case E2 is divided into two parts, the upper part is the molten salt-gravel solid block, and

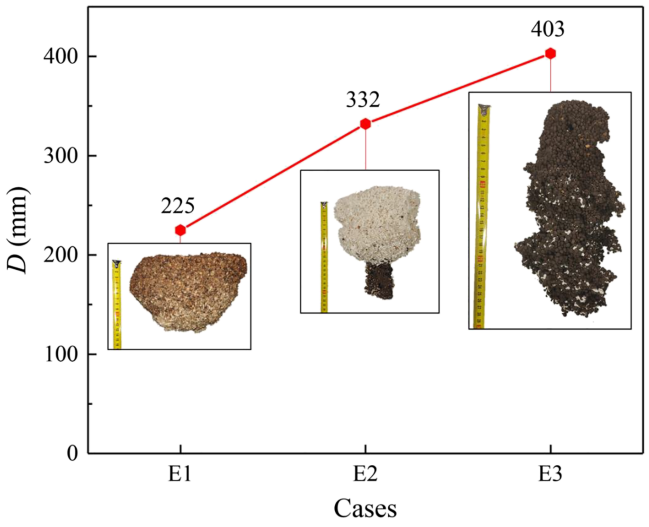

FIGURE 12 Seepage depths of molten salt in multi-layer fillers

the lower part is the molten salt-LECA solid block. It can be seen that a small amount of molten salt seeps into the LECA layer. Nevertheless, the solid block of case E3 is that the solidification of the molten salt entirely occurs in the LECA layer. The seepage depth is reduced by 79 mm compared with case A1 because the molten salt conducts intense heat transfer with the sand and gravel during seepage, and the molten salt cools relatively quickly in the sand and gravel layers. Eventually, the solidification position of the molten salt is advanced, and the seepage depth is reduced. But this is still a high value that accounts for 58.3% of the total height of the foundation. It can be concluded that if a molten salt leakage accident occurs in the practical storage tank, the seepage depth of molten salt in the foundation is tremendous. And it is complicated to deal with the accident. Therefore, it may be necessary to study how to block the seepage of molten salt, and this is desirable for future work.

4 | CONCLUSIONS

In this paper, an experimental study on the seepage of leaked molten salt in foundation fillers with different configurations was carried out. The obtained results are summarized below.

1. At the operating temperature of 565°C, when LECA, sand, and gravel are used as foundation fillers, the average temperatures of each layer of the tank foundation fillers are 131.73°C, 141.91°C, and 149.27°C, respectively. LECA can be preferentially selected as the thermal insulation materials of the tank foundation.
2. Seepage depth of molten salt in foundation fillers increases with the operating temperature. When the operating temperature increases from 290°C to 565°C, the seepage depth of molten salt in LECA, sand, and gravel increases by 1.47, 1.08, and 2.07 times, respectively. Therefore, the foundation design of the hot tank deserves more attention to prevent the contamination range from being too large after the leakage.
3. At the same operating temperature, the seepage depth of molten salt in sand and gravel is significantly lower than that in LECA. Moreover, the thicker the LECA layer and the thinner the sand or gravel layer, the greater the seepage depth. To increase the strength of the foundation, reduce the pollution range of the leaked molten salt, and reduce the difficulty of accident handling, the thickness of the sand and gravel layer should be appropriately increased when designing the tank foundation.

Future research should focus on accurate detection and seepage blocking of leaked molten salt to provide a guarantee for the safe operation of molten salt TESS in CSP plants. The results in this paper provide a good starting point for discussion.

ACKNOWLEDGEMENTS

This work was supported by the National Natural Science Foundation of China (52036008).

DECLARATION OF COMPETING INTEREST

The authors declare that they have no known competing financial interests or personal relationships that could have appeared to influence the work reported in this paper.

NOMENCLATURE

a	thickness of the sand layer (mm)
b	thickness of the gravel layer (mm)
c	thickness of the LECA layer (mm)
D	seepage depth (mm)
d	distance between the top of the solid block and the top of the fillers (mm)
T_{op}	operating temperature (°C)
T	temperature (°C)
t	time (s, min, h)
W	maximum seepage width (mm)
y	depth position of fillers (mm)

ORCID

Hao Zhou https://orcid.org/0000-0001-9779-7703

REFERENCES

1. Li B, Haneklaus N. The role of clean energy, fossil fuel consumption and trade openness for carbon neutrality in China. *Energy Rep*. 2022;8:1090-1098. doi:10.1016/j.egyr.2022.02.092
2. Zhang L, Du Q, Zhou D, Zhou P. How does the photovoltaic industry contribute to China's carbon neutrality goal? Analysis of a system dynamics simulation. *Sci Total Environ*. 2022;808:151868. doi:10.1016/j.scitotenv.2021.151868
3. Zhao X, Ma X, Chen B, Shang Y, Song M. Challenges toward carbon neutrality in China: strategies and countermeasures. *Resour Conserv Recycl*. 2022;176(October 2021):105959. doi:10.1016/j.resconrec.2021.105959
4. Liu T, Yang J, Yang Z, Duan Y. Techno-economic feasibility of solar power plants considering PV/CSP with electrical/thermal energy storage system. *Energ Conver Manage*. 2022;255(February):115308. doi:10.1016/j.enconman.2022.115308
5. Binder M, Schuhbauer C, Uhlig R, Schwarzbözl P, Schwaiger R, Pitz-Paal R. Comparison of different safety concepts for evaluation of molten salt receivers. *Sol Energy*. 2022;234(February):119-127. doi:10.1016/j.solener.2022.01.051
6. IRENA. *Power Generation Costs in 2020*; 2021. https://www.irena.org/-/media/Files/IRENA/Agency/Publication/2021/Jun/IRENA_Power_Generation_Costs_2020.pdf
7. Aseri TK, Sharma C, Kandpal TC. Estimation of capital costs and techno-economic appraisal of parabolic trough solar collector and solar power tower based CSP plants in India for different condenser cooling options. *Renew Energy*. 2021;178:344-362. doi:10.1016/j.renene.2021.05.166
8. Herrmann U, Kelly B, Price H. Two-tank molten salt storage for parabolic trough solar power plants. *Energy*. 2004;29(5-6):883-893. doi:10.1016/S0360-5442(03)00193-2
9. Zaversky F, García-Barberena J, Sánchez M, Astrain D. Transient molten salt two-tank thermal storage modeling for CSP performance simulations. *Sol Energy*. 2013;93:294-311. doi:10.1016/j.solener.2013.02.034
10. Rodríguez I, Pérez-Segarra CD, Lehmkuhl O, Oliva A. Modular object-oriented methodology for the resolution of molten salt storage tanks for CSP plants. *Appl Energy*. 2013;109:402-414. doi:10.1016/j.apenergy.2012.11.008
11. Suárez C, Iranzo A, Pino FJ, Guerra J. Transient analysis of the cooling process of molten salt thermal storage tanks due to standby heat loss. *Appl Energy*. 2015;142:56-65. doi:10.1016/j.apenergy.2014.12.082
12. Bonilla J, Rodríguez-García MM, Roca L, de la Calle A, Valenzuela L. Design and experimental validation of a computational effective dynamic thermal energy storage tank model. *Energy*. 2018;152:840-857. doi:10.1016/j.energy.2017.11.017
13. Araújo AKA, Medina TGI. Analysis of the effects of climatic conditions, loading level and operating temperature on the heat losses of two-tank thermal storage systems in CSP. *Sol Energy*. 2018;176(October):358-369. doi:10.1016/j.solener.2018.10.020
14. Torras S, Pérez-Segarra CD, Rodríguez I, Rigola J, Oliva A. Parametric study of two-tank TES systems for CSP plants. In: *Energy Procedia*. Vol.69. Elsevier Ltd; 2015:1049-1058. doi:10.1016/j.egypro.2015.03.206.
15. Price H, Mehos M, Kearney D, et al. Concentrating solar power best practices. *Conc Sol Power Technol*. 2021(June):725-757. doi:10.1016/b978-0-12-819970-1.00020-7
16. Zhou H, Shi H, Zhang J, Zhou M. Experimental and numerical investigation of temperature distribution and heat loss of molten salt tank foundation at different scales. *Heat Mass Transf*. 2020;56(10):2859-2869. doi:10.1007/s00231-020-02905-x
17. Zhou H, Wang Z, Zhou M, Xu J. Thermal properties, permeability and compressive strength of highly porous accumulated ceramsites in the foundation of salt tank for concentrate solar power plants. *Appl Therm Eng*. 2020;164:114451. doi:10.1016/j.applthermaleng.2019.114451
18. Wan Z, Wei J, Qaisrani MA, Fang J, Tu N. Evaluation on thermal and mechanical performance of the hot tank in the two-tank molten salt heat storage system. *Appl Therm Eng*. 2020;167(January 2019):114775. doi:10.1016/j.applthermaleng.2019.114775
19. Zhou H, Shi H, Lai Z, Zuo Y, Hu S, Zhou M. Migration and phase change study of leaking molten salt in tank foundation material. *Appl Therm Eng*. 2020;170:114968. doi:10.1016/j.applthermaleng.2020.114968
20. Shi H, Zhou H, Ma PN. et al. Experimental investigation of migration and solidification of molten salt leaking through tank cracks. *J Zhejiang Univ Sci A*. 2021;22(12):979-991. doi:10.1631/jzus.A2100011
21. Wang ZW, Zhou H, Luo JW, Wu QW, Cen KF. Research on thermal conductivity of storage tank foundation materials after molten salt leakage. *J Zhejiang Univ (Engineering Sci)*. 2022;56(1):137-143. doi:10.3785/j.issn.1008-973X.2022.01.015
22. Turchi CS, Vidal J, Bauer M. Molten salt power towers operating at 600–650°C: salt selection and cost benefits. *Sol Energy*. 2018;164(November 2017):38-46. doi:10.1016/j.solener.2018.01.063
23. Roper R, Harkema M, Sabharwall P, et al. Molten salt for advanced energy applications: a review. *Ann Nucl Energy*. 2022;169:108924. doi:10.1016/j.anucene.2021.108924
24. Woodside W, Messmer JH. Thermal conductivity of porous media. II Consolidated rocks. *J Appl Phys*. 1961;32(9):1699-1706. doi:10.1063/1.1728420
25. Woodside W, Messmer JH. Thermal conductivity of porous media. I Unconsolidated sands. *J Appl Phys*. 1961;32(9):1688-1699. doi:10.1063/1.1728419
26. Zhou H, Wang Z, Zhou M, Cen K. Experimental measurements and XCT based simulation of effective thermal conductivity of stacked ceramsites in molten-salt tank foundation. *Heat Mass Transf*. 2019;55(11):3103-3115. doi:10.1007/s00231-019-02646-6

How to cite this article: Zhang M, Zuo Y, Yu X, Zhang A, Zhou H. Experimental study on seepage flow characteristics of leaked molten salt in foundation fillers in concentrating solar power plants. *Asia-Pac J Chem Eng*. 2022;17(5):e2813. doi:10.1002/apj.2813